Electronic Supplementary Material (ESI) for Physical Chemistry Chemical Physics.

Supporting Information: Reproducibility and Stability of Silane Layers in Nanoconfined Electrochemical Systems

Dominik Duleba, Shekemi Denuga, Robert P. Johnson*

School of Chemistry, University College Dublin, Belfield, Dublin 4, Ireland
nanopore, nanopipette, surface modification, silane, APTES, APTMS, stability

*robert.johnson@ucd.ie

Contents

STEM imaging

Figure S1 shows a representative STEM image of a nanopipette fabricated using the Sutter parameters indicated in the experimental section. The pore size (circa 60 nm diameter), the walls, the internal cone angle, and the filament are clearly visible.

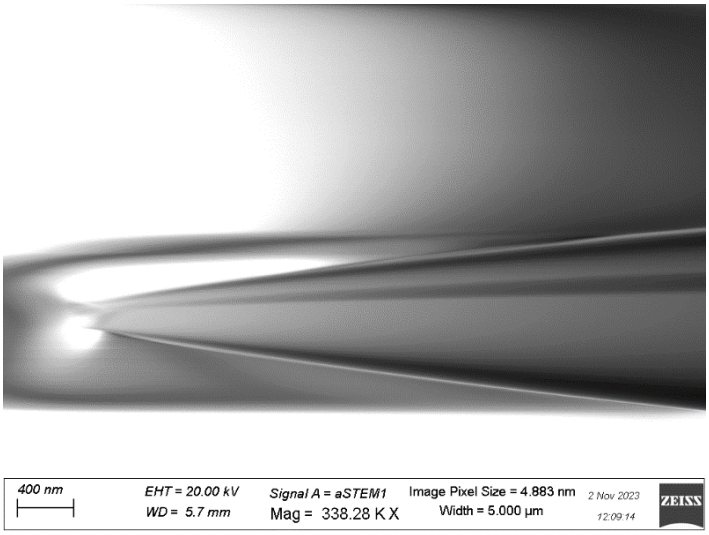

Figure S1. STEM image of a nanopipette pulled with the parameters used in this study. (Line 1: H700 F4 V20 D170 P0, Line 2: H680 F4 V50 D170 P200).

Nanopipette blockage/dewetting

Figure S2 shows the case where the conductance of the nanopipette is lost due to the blockage/dewetting of the pore, as well as the case when conductance is retained. The conductance is related to the gradient of the curves at zero applied potential. The gradient changes towards zero on Figure S2A, while the gradient is stable on Figure S2B.

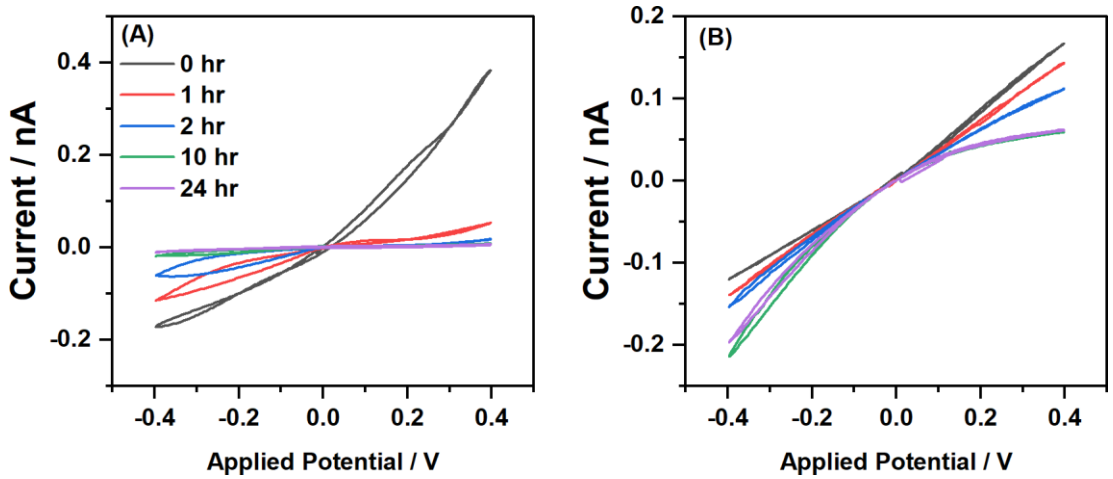

Figure S2. (A) Current-voltage curves over time for a nanopipette functionalized with 5% APTES in EtOH and becomes blocked/dewetted, as well as (B) a nanopipette functionalized with vapor-deposited APTES which remains open over 24 hours.

The symmetry of the logarithmic rectification ratio

To demonstrate the better symmetry of logRR compared to regular RR, a simple Finite Element Model was used to simulate the logarithmic and regular rectification ratios for different surface charge densities. The finite element model is based on the Nernst-Planck-Poisson-Navier-Stokes equations and is the same as reported by us previously.[1] Figure S3 shows that logRR is more symmetric above and below the transition from having its ON-state and the positive applied potential and having its ON-state at the negative applied potential. A transition from a state of -5 mC m^{-2} to 0 mC m^{-2} surface charge density leads to the same logRR change as a transition from 0 mC m^{-2} to +5 mC m^{-2}. This is not the case for the regular RR. As such, when monitoring the continuous transition of silanated nanopipettes from a positively charged nanopipette to a negatively charged nanopipette, logRR is better for comparison. It should be noted that Souna et al.,[2] have also been utilized a different metric with the same purpose of providing a symmetry in the RR response. For the data we report here, this previously reported metric was not suitable as it goes to infinity when the nanopore switches its ON-state to the other potential, rather than smoothly crossing over at zero.

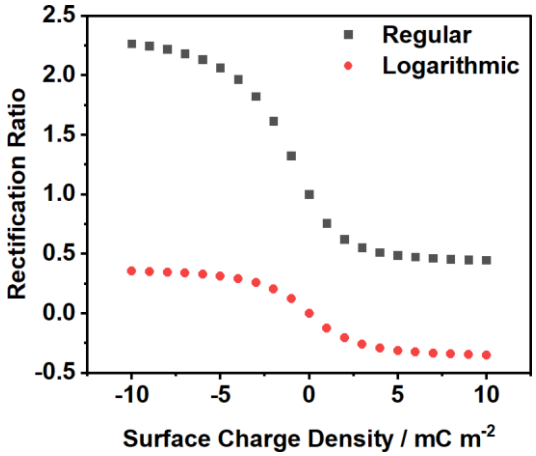

Figure S3. Simulated regular and logarithmic rectification ratios as a function of the nanopipette surface charge density.

Contact Angle Measurements

Contact angle measurements have been previously utilized to evaluate the stability of silanes deposited on planar silicon wafers at anhydrous conditions.[3] We also use contact angle measurements to evaluate the stability of liquid-phase and vapor-phase deposited silanes. Table S1 shows the contact angles before and after exposure to 1 mM KCl for 24 hours. The contact angles of liquid-phase deposition are greater than those of vapor-phase, which can be attributed to silane clusters at areas of high surface roughness where amine moieties do not fully orient outwards, exposing their hydrophobic alkyl chains.[4,5] In contrast, the smooth and homogeneous topography produced by vapor-phase deposition tends to orient the amine group outwards.[4,5] The magnitude of the initial contact angles for both the unmodified and silanized wafers are comparable to previous reports.[6–8] When exposed to the electrolyte for 24 hours, the contact angle does not change for the unmodified quartz wafers, however, the contact angles decrease for all silane functionalized surfaces. A decrease of the contact angle indicates an increase of the surface hydrophilicity which is the expected outcome when a silanized hydrophobic surface is changing towards the hydrophilic surface expected from bare quartz. According to the contact angle measurements, the most stable modification is triple vapor-deposited APTES. It should be noted that while considering the contact angles is useful, the stability on a planar quartz surface is not fully comparable to the stability in our nanoconfined nanopipettes. The silane layers on the planar quartz surface do not experience the electric fields (and hence the electric migrative and electroosmotic forces) and local concentration polarization that the nanopipettes experience during the electrochemical measurement. For practical purposes, the stability during electrochemical measurements is most relevant.

Table S1. Contact Angle (CA) measurements of unmodified and silanized planar quartz slides before and after exposure to 1 mM KCl for 24 hours. Sample images of contact angles are provided in Figure S4.

Method	**CA / deg (0 hour)**	**CA / deg (24 hour)**	**ΔCA /deg**
Unmodified	31±1	31.8±0.6	0±2
APTMS EtOH	63.9±0.6	51.8±0.5	-12±1
APTES EtOH	66.9±0.9	52.6±2	-14±2
APTMS CVD	56±1	42±2	-15±3
APTES CVD	56±1	44±2	-13±3
APTES 3x CVD	59±2	54±1	-5±3

Representative images of the contact angle droplets for some of the surfaces are given in Figure S4. The fitting of the droplet that is used for the calculation of the contact angles is also shown.

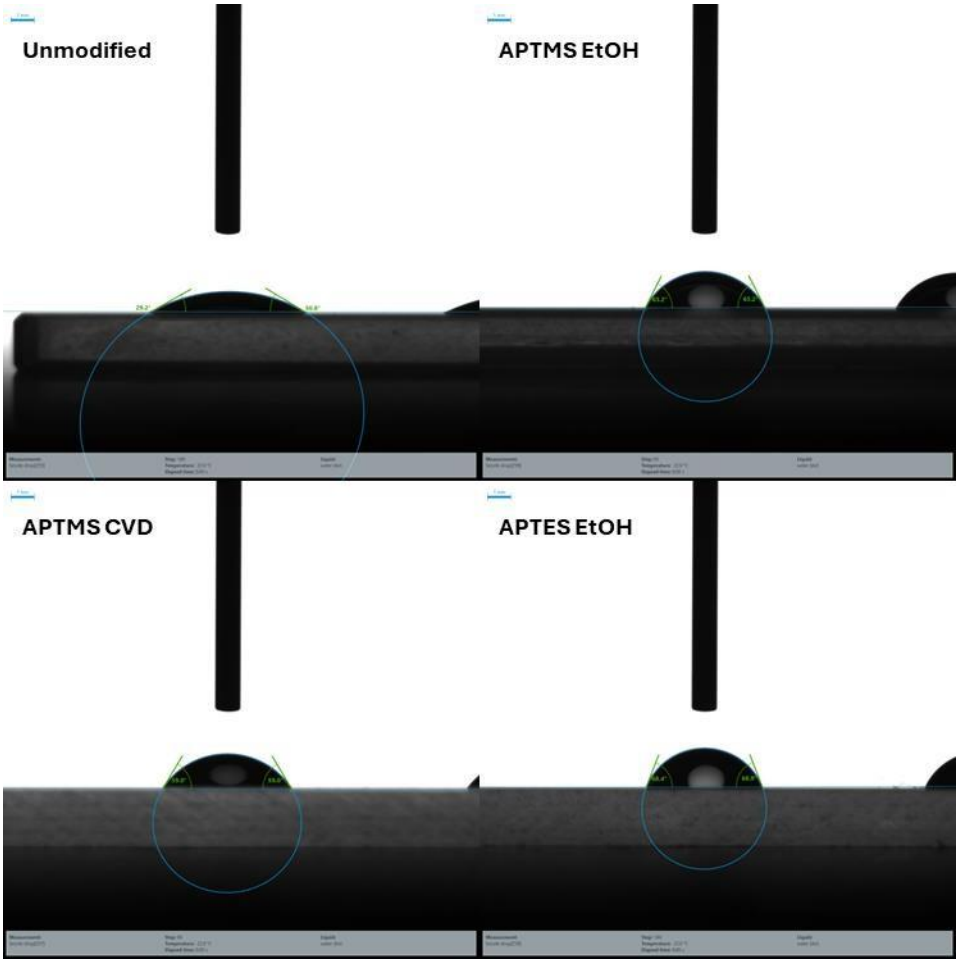

Figure S4. Contact Angle Images.

Electrochemical Monitoring of Silane Desorption/Rearrangement

For more transparency about what the data shown in Figure 4 in the main paper looks like, representative logRR and ΔlogRR traces for individual nanopipettes silanized with each silanization method are provided is Figures S5-S8. At least 5 such curves are averaged out to yield the results shown in the main paper.

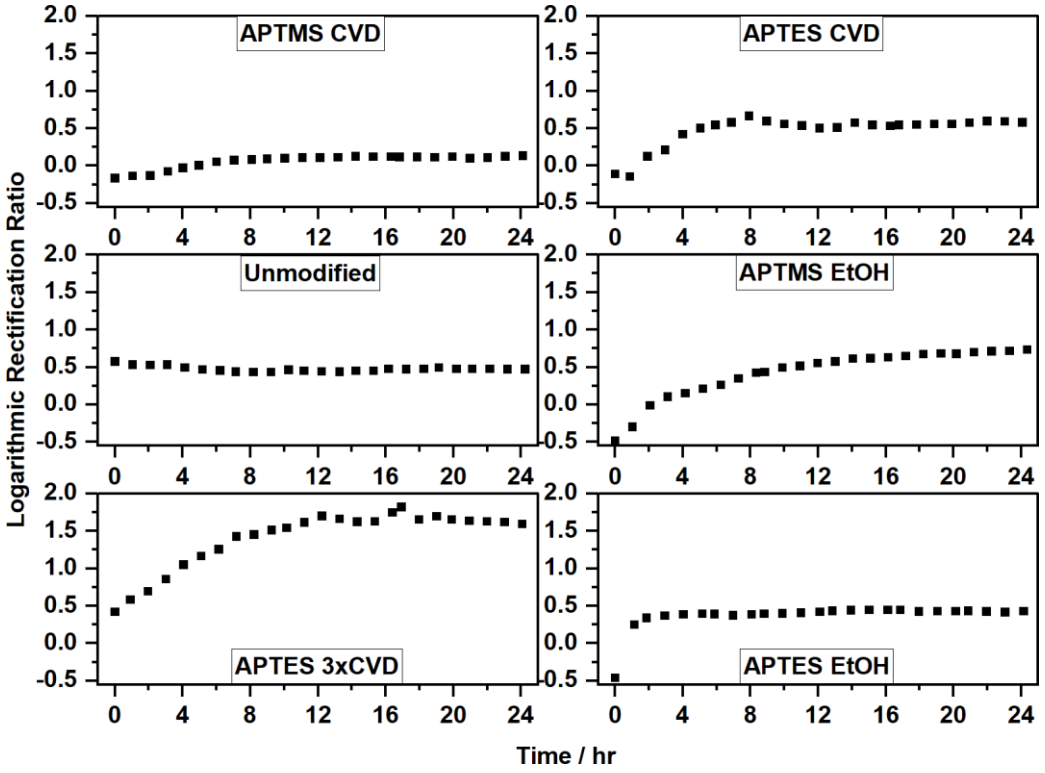

Figure S5. Sample plots of the logarithmic rectification ratio as a function of time for individual nanopipettes.

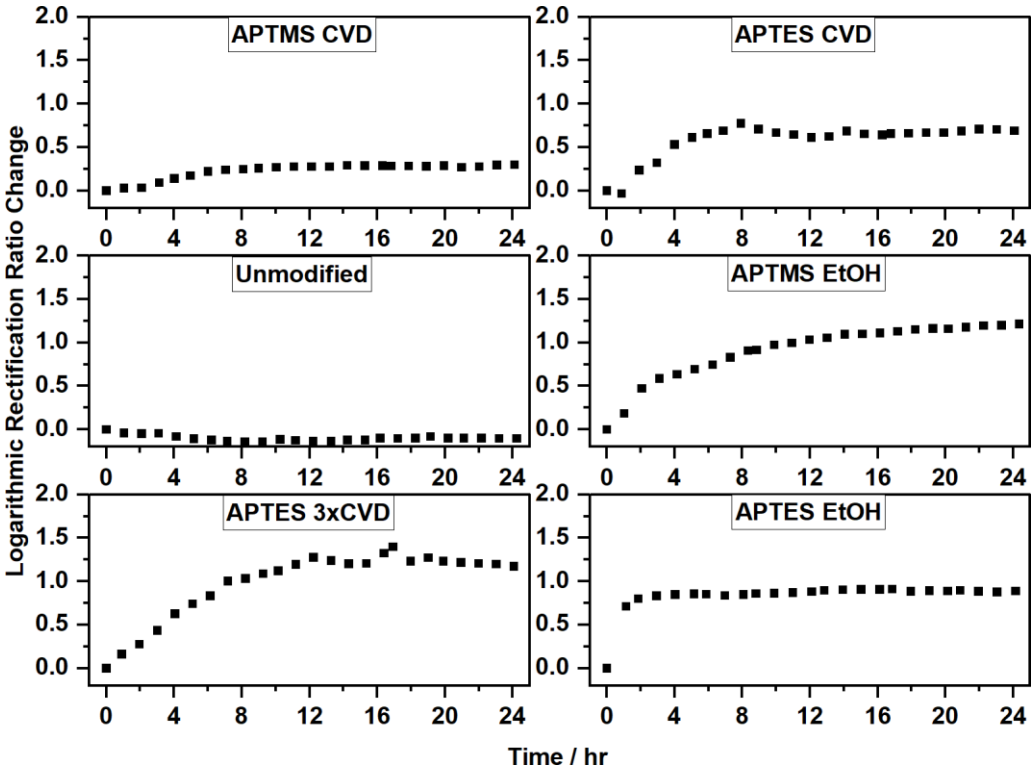

Figure S6. Sample plots of the change of logarithmic rectification ratio as a function of time for individual nanopipettes.

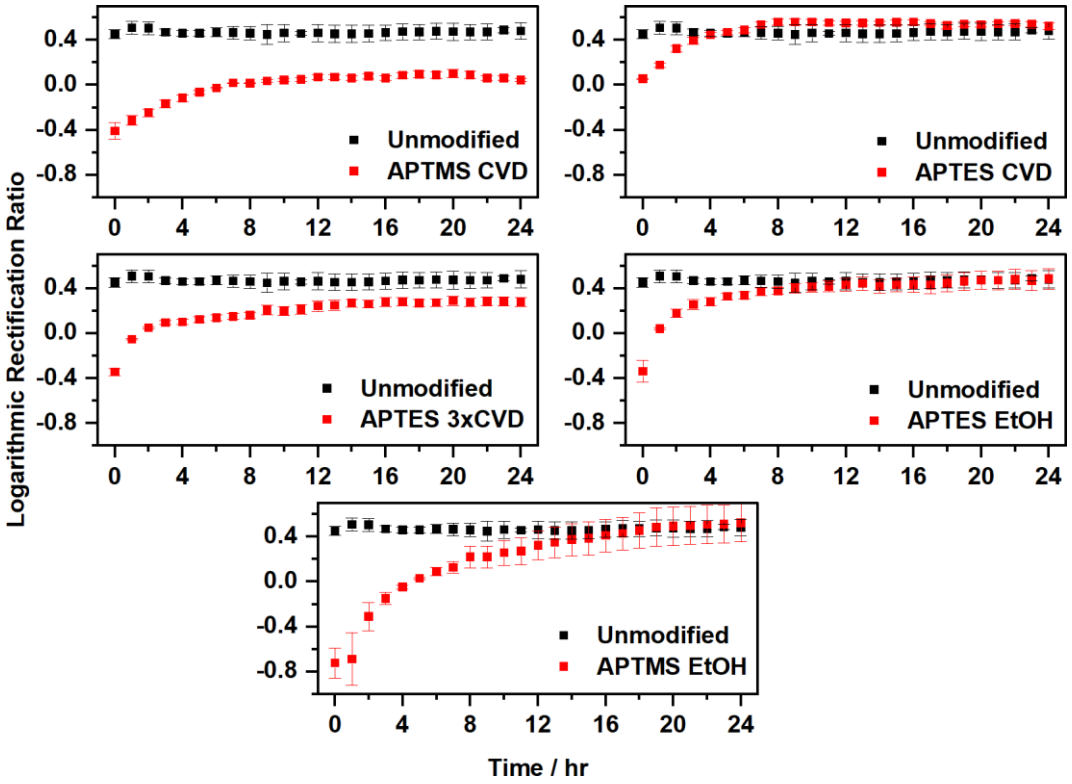

Figure S7. Comparison of the evolution of the logarithmic rectification ratio of each silane modification to the unmodified nanopipettes. Each curve is the average of at least 5 nanopipette measurements.

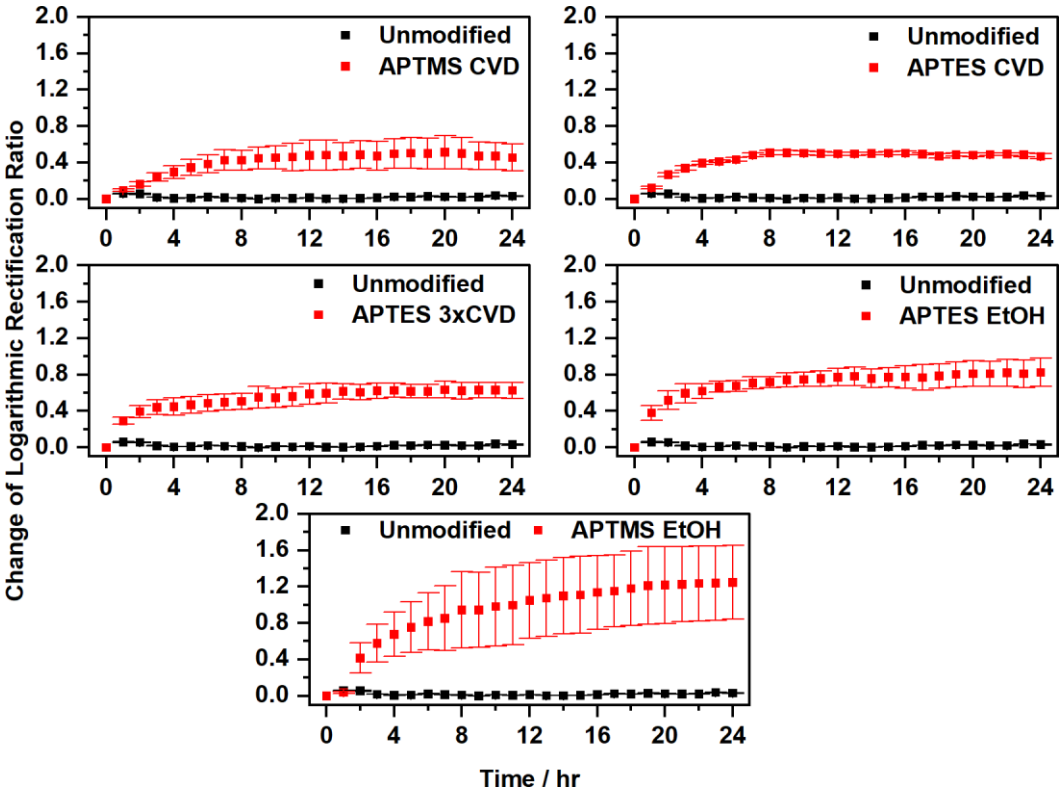

Figure S8. Comparison of the evolution of the logarithmic rectification change of each silane modification to the unmodified nanopipettes. Each curve is the average of at least 5 nanopipette measurements.

References

(1) Duleba, D.; Dutta, P.; Denuga, S.; Johnson, R. P. Effect of Electrolyte Concentration and Pore Size on Ion Current Rectification Inversion. *ACS Measurement Science Au*, 2022, *2*, 271–277.

(2) J. Souna, A.; H. Motevaselian, M.; W. Polster, J.; D. Tran, J.; S. Siwy, Z.; R. Aluru, N.; T. Fourkas, J. Beyond the Electrical Double Layer Model: Ion-Dependent Effects in Nanoscale Solvent Organization. *Phys. Chem. Chem. Phys.* **2024**, *26* (8), 6726–6735. https://doi.org/10.1039/D3CP05712G.

(3) Zhu, M.; Lerum, M. Z.; Chen, W. How to Prepare Reproducible, Homogeneous, and Hydrolytically Stable Aminosilane-Derived Layers on Silica. *Langmuir*, 2012, *28*, 416–423.

(4) Fiorilli, S.; Rivolo, P.; Descrovi, E.; Ricciardi, C.; Pasquardini, L.; Lunelli, L.; Vanzetti, L.; Pederzolli, C.; Onida, B.; Garrone, E. Vapor-Phase Self-Assembled Monolayers of Aminosilane on Plasma-Activated Silicon Substrates. *J. Colloid Interface Sci.* **2008**, *321* (1), 235–241. https://doi.org/10.1016/j.jcis.2007.12.041.

(5) Song, X.; Zhai, J.; Wang, Y.; Jiang, L. Self-Assembly of Amino-Functionalized Monolayers on Silicon Surfaces and Preparation of Superhydrophobic Surfaces Based on Alkanoic Acid Dual Layers and Surface Roughening. *J. Colloid Interface Sci.* **2006**, *298* (1), 267–273. https://doi.org/10.1016/j.jcis.2005.11.048.

(6) Yadav, A. R.; Sriram, R.; Carter, J. A.; Miller, B. L. Comparative Study of Solution Phase and Vapor Phase Deposition of Aminosilanes on Silicon Dioxide Surfaces. *Mater. Sci. Eng. C Mater. Biol. Appl.* **2014**, *35*, 283–290. https://doi.org/10.1016/j.msec.2013.11.017.

(7) Janczuk, B.; Zdziennicka, A. A Study on the Components of Surface Free Energy of Quartz from Contact Angle Measurements. *J. Mater. Sci.* **1994**, *29* (13), 3559–3564. https://doi.org/10.1007/BF00352063.

(8) Iglauer, S.; Salamah, A.; Sarmadivaleh, M.; Liu, K.; Phan, C. Contamination of Silica Surfaces: Impact on Water–CO2–Quartz and Glass Contact Angle Measurements. *Int. J. Greenh. Gas Control* **2014**, *22*, 325–328. https://doi.org/10.1016/j.ijggc.2014.01.006.